Korean J. Chem. Eng., 39(8), 2080-2088 (2022)
DOI: 10.1007/s11814-022-1093-4

pISSN: 0256-1115
eISSN: 1975-7220

Preparation of N and Eu doped TiO_2 using plasma in liquid process and its photocatalytic degradation activity for diclofenac

Heon Lee*,‡, Young-Kwon Park,‡, and Sang-Chul Jung*,†**

*Department of Environmental Engineering, Sunchon National University, Sunchon 57922, Korea
**School of Environmental Engineering, University of Seoul, Seoul 02504, Korea
(*Received 5 January 2022 • Revised 19 February 2022 • Accepted 23 February 2022*)

Abstract−Pharmaceutical contaminants such as diclofenac (DCF) cannot be removed in existing wastewater treatment facilities; therefore, studies on application of new treatment processes and improvement of efficiency are required. In this study, a modified photocatalyst doped with nitrogen and europium was prepared and the performance of DCF was evaluated. A modified photocatalyst that responds to visible light was prepared by precipitating nitrogen and europium in a TiO_2 powder using a plasma-in-liquid process (PLP). The performance of the photocatalyst was evaluated by a degradation experiment of diclofenac, a pharmaceutical ingredient. The dopant tended to precipitate in proportion to the amount of precursor added, but more nitrogen precipitated than europium even when the same amount was added. Nitrogen and europium were dispersed evenly throughout the TiO_2 powder, and the Ti2p peak position of the modified TiO_2 photocatalyst (MTP) coincided with bare TiO_2, and europium precipitated in the form of Eu_2O_3. The bandgap energy of the MTPs was lower than that of unmodified TiO_2 photocatalyst, but the MTP with only europium precipitated was the lowest. When a blue light source in the visible region was used, DCF decomposition by MTPs was improved by about 15 to 25 times compared to bare TiO_2, and europium precipitation photocatalyst had the highest DCF decomposition characteristic. In addition, MTPs showed excellent reusability properties. Four kinds of by-products were detected in the decomposition process of DCF, and three decomposition pathways by reactions such as decarboxylation, C-N cleavage and hydroxylation were considered. The final mineralization to H_2O, CO_2, and chlorine occurs by hydroxylation, such as by OH, on the MTP.

Keywords: Visible Light-responsive Photocatalyst, Plasma in Liquid Process, Nitrogen, Europium, Diclofenac

INTRODUCTION

In many countries, drugs are abused, resulting in many unused stock drugs that cannot be treated adequately and are discarded, polluting the environment in various ways [1-3]. Diclofenac (DCF) is widely used for the treatment of inflammation and pain such as gout, but due to its stable chemical structure, it is not removed by the traditional wastewater treatment process and is detected in aquatic environments such as surface water and ground water [4-6]. DCF present in water has low acute toxicity, but it can act as a dangerous influencing factor by generating bacteria resistant to drugs and adversely affecting the aquatic ecosystem [6]. Therefore, a new process is needed to decompose pharmaceutical agents effectively, such as diclofenac, which traditional water treatment methods cannot degrade. For this purpose, research has been conducted to apply various advanced oxidation processes (AOPs) such as photocatalysis, UV-persulfate, photo-Fenton, and electrochemical oxidation [6-9]. On the other hand, it has problems such as complicated devices, low efficiency, and secondary pollution.

The decomposition process of organic matter using TiO_2 photocatalyst has been studied and applied [10-12]. Although the TiO_2 photocatalytic process is easy and does not generate secondary waste, it can only be used in the ultraviolet region [13]. The most widely used, anatase TiO_2, has a bandgap of 3.2 eV, meaning that it becomes active as a photocatalyst in the ultraviolet region with a wavelength of 388 nm or less. Therefore, to be used widely in real life, the bandgap of the TiO_2 photocatalyst needs to be reduced to achieve high photoactivity in the visible region. Doping the surface is a widely used method of reducing the bandgap of TiO_2. Numerous studies and applications have been reported to prepare TiO_2 photocatalysts that react to visible light by doping with specific metals, nitrogen, and carbon [14-16].

Various methods have been used to dope metal and non-metal elements in TiO_2 powder, but the plasma-in-liquid process (PLP) has attracted recent attention [17-19]. PLP has been applied to various fields such as water treatment and nanoparticle synthesis owing to its easy and straightforward process [20-22]. In particular, a substrate can be doped with various elements in a one-step process [23-25].

In this study, TiO_2 was precipitated with nitrogen and europium using PLP to prepare a photocatalyst that reacts to a wide wavelength range. The physical, chemical and optical singularities of the prepared modified TiO_2 photocatalysts (MTPs) were investigated using several instrument analyzers. The photocatalytic efficiency of the prepared MTPs in visible and ultraviolet light was then com-

†To whom correspondence should be addressed.
E-mail: jsc@sunchon.ac.kr
‡Co-first authors.

pared with that of the bare TiO_2 photocatalyst.

EXPERIMENTAL

1. Materials

For the TiO_2 photocatalyst, P-25 purchased from Evonik Aeroxide was used. Ammonium chloride (NH_4Cl) and europium(III) chloride hexahydrate ($EuCl_3 \cdot 6H_2O$), the precursors of nitrogen (N) and europium (Eu) as dopants, were purchased from Sigma-Aldrich. As the PLP reactant aqueous solution, deionized water (electrical conductivity ≤2 μS/cm) manufactured by Daejung Metal & Chemical was used. Diclofenac, the decomposition target, was used in the form of the diclofenac sodium salt (DCF, $C_{14}H_{10}Cl_2NNaO_2$) from Sigma Aldrich.

2. Preparation of MTP

The preparing process of nitrogen doped TiO_2 (N-TiO_2), europium doped TiO_2 (Eu-TiO_2) and nitrogen/europium co-doped TiO_2 (N/Eu-TiO_2) using PLP reaction was as follows. Bare TiO_2 powder

Table 1. The chemical composition of bare TiO_2 and modified TiO_2 photocatalysts prepared by PLP

Photocatalyst	Precursor conc. (mM)		Titanium (Ti)		Oxygen (O)		Nitrogen (N)		Europium (Eu)	
	NH_4Cl	$Eu(Cl)_3$	wt%	at%	wt%	at%	wt%	at%	wt%	at%
Bare TiO_2	0	0	59.7	33.1	40.3	66.9	0.0	0.0	0.0	0.0
N-TiO_2	10	0	58.2	31.6	39.2	63.7	2.6	4.7	0.0	0.0
Eu-TiO_2	0	10	58.4	32.9	39.5	66.7	0.0	0.0	2.1	0.4
N-Eu-TiO_2	5	5	58.2	32.2	39.2	65.0	1.4	2.6	1.2	0.2

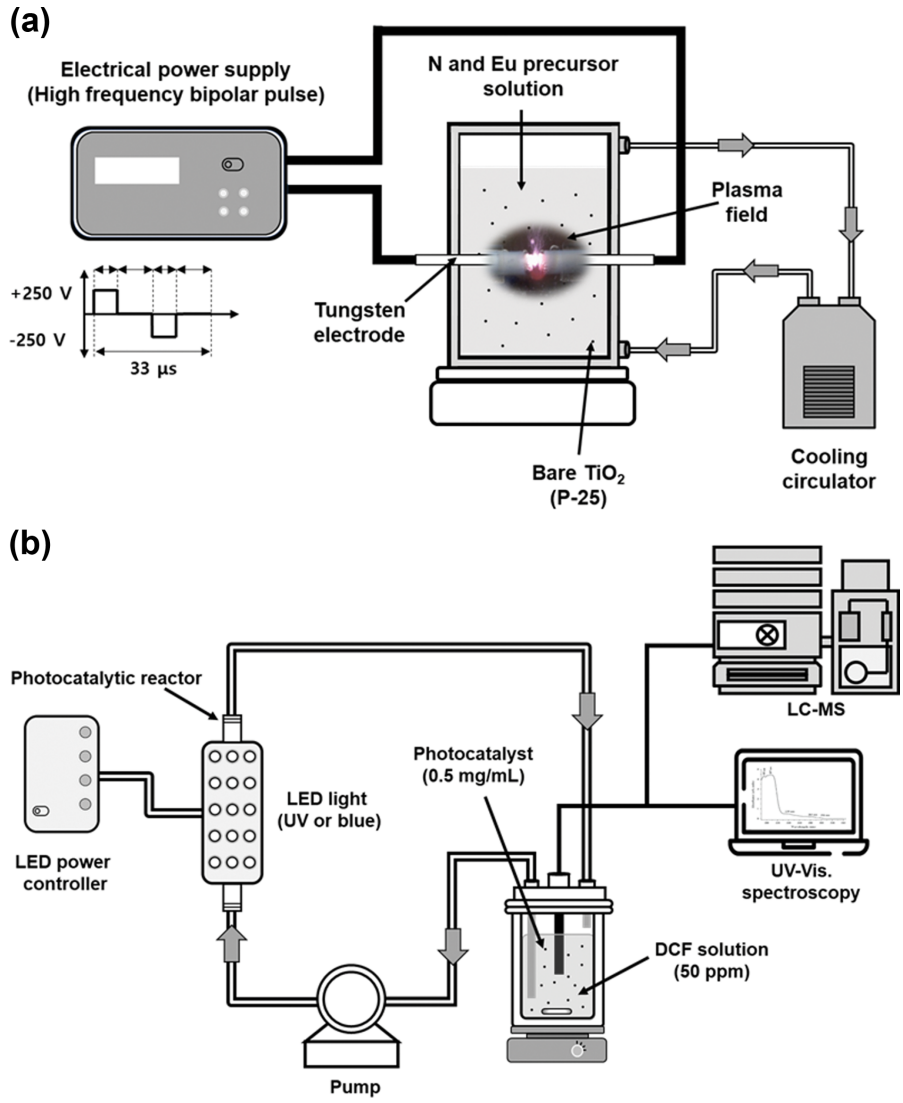

Fig. 1. PLP system for the synthesis of modified photocatalysts (a) and photolysis system for DCF decomposition (b).

(0.5 g) was added to deionized water (250 ml) and stirred, followed by sonication for one minute. In the reaction solution to which TiO_2 powder was added, ammonium chloride and europium chloride as precursors were dissolved at concentrations (5 mM or 10 mM), and the total concentration of the precursor was maintained at 10 mM in all experiments. Table 1 shows the concentration conditions of the precursors used in the preparation of MTPs in this study. After transferring the prepared reactant solution to the PLP reactor, power was supplied to dope the TiO_2 with nitrogen and europium through a plasma reaction. After the plasma reaction was completed, the reactants were washed and centrifuged to separate unreacted substances. The final product was obtained by filtration and dried in a dryer at 373 K for 10 hours. Fig. 1(a) shows the configuration of the PLP system used to prepare MTPs by precipitating N and Eu. The reaction solution in which TiO_2 and precursor are mixed is filled inside the double tube type reactor located in the center of the figure. Electrical energy is supplied through the tungsten electrodes installed on both sides of the reactor, and plasma reaction is formed to precipitate N and Eu on the TiO_2 surface. The electrical operation parameters of the power supply shown on the left of the figure were kept constant at 250 V, 30 kHz, and 5 μs. Since the heat generated by the plasma reaction causes the temperature of the reaction solution to rise, the temperature was kept constant by using a cooling circulator.

Individual element distribution and morphology of modified TiO_2 photocatalysts prepared by PLP were observed using high resolution field emission transmission electron microscopy (HR-FETEM, JEOL-JEM-2100F). X-ray photoelectron spectroscopy (XPS, SSK-Multilab 2000) was used to measure the elemental chemical state, bond formation, and chemical composition of modified TiO_2 photocatalysts. The band gap energy, a representative characteristic of photocatalysts, was calculated through UV-Vis diffuse reflectance spectra (DRS) spectra obtained using a UV-Vis spectrometer (Shimadzu, UV-2450).

3. Assessment of MTPs Activity

The photocatalytic performance of the prepared MTPs was measured by the decomposition of DCF, a pharmaceutical ingredient, and was compared with the unmodified TiO_2 powder. Fig. 1(b) shows the configuration diagram of the photolysis device for the DCF decomposition reaction; a detailed description is described elsewhere [15,18]. The light source of the photolysis reaction was a UV light module (λmax=375 nm, total power dissipation: 8 W) and a blue light module (λmax=465 nm, total power dissipation: 12 W) manufactured using light-emitting diodes (LEDs).

The photocatalytic performance of the modified TiO_2 photocatalysts was evaluated using the following method. After preparing 600 mL of 50 ppm DCF solution, the MTP or bare TiO_2 photocatalyst was added at a concentration of 0.5 mg/mL and stirred to disperse uniformly in a DCF solution. The reaction solution to which the MTPs were added was transferred to the PLP reactor and circulated uniformly throughout the photolysis device for 10 minutes in a state where no light was supplied. Using a light source controller, the DCF decomposition reaction was caused by irradiation with UV light and blue light, and the decomposed reactant solution was analyzed at specific times. The recovered reaction solution was centrifuged and filtered to remove MTPs, and the DCF concentration was calculated using a spectrophotometer. The decomposition rate was calculated by measuring the absorbance of DCF at 276 nm in the reaction solution after the degradation reaction was completed. Liquid chromatography with a mass spectrometer (LC-MS, Shimadzu LC-MS 2020) was used to detect by-products produced during the DCF degradation reaction. Chromatic separation was performed using a VPODS C18 column, and the operation was conducted in negative ESI mode.

RESULTS AND DISCUSSION

1. Characterization of the MTP

The TiO_2 powders modified by PLP were observed by high resolution-field emission transmission electron microscopy (HR-FETEM), as shown in Fig. 2. Fig. 2(a) presents a real image of the observed MTP, and the particle size was 15-40 nm. Fig. 2(b), (c), and (d) presents mapping images of Ti, N, and Eu, and the dots representing each element are expressed in the same form as the actual image in Fig. 2(a). Ammonium ions (NH_4^+) and europium ions (Eu^{3+}) generated in the reaction solution by dissociation of the dopant precursor are reduced by many electrons in the PLP and deposited on the TiO_2 powder [26-28]. From these TEM observation results, the TiO_2 powder modified with PLP in this study contained nitrogen and europium precipitated uniformly in the TiO_2 powder.

The chemical composition and chemical state of MTP prepared by PLP were examined by X-ray photoelectron spectroscopy (XPS). The results are shown in Fig. 3 as a high-resolution XPS spectrum for Ti, O, N, and Eu. Fig. 3(a) shows the XPS narrow spectrum of the Ti2p region of MTP with bare TiO_2. Peaks due to $Ti2p_{3/2}$ and $Ti2p_{1/2}$ in bare TiO_2 and MTP were observed at binding energies (BE) of 464.1 eV and 458.4 eV. Spin-orbit splitting between $Ti2p_{3/2}$ and $Ti2p_{1/2}$ was 5.7 eV, indicating a peak due to Ti^{4+} of TiO_2 [29-31]. On the other hand, because the Ti2p peak positions of bare TiO_2 and MTP coincide, the crystal of TiO_2 does not change because of PLP, and it can be assumed that nitrogen and europium precipitated on the surface of the TiO_2 powder. Two peaks were observed in the O1s region of Fig. 3(b). The peak at 530.2 eV was assigned to Eu-O and Ti-O because the BE of Eu-O bonds and BE of Ti-O bonds coincide [32]. The peak of 532.2 eV was due to the hydroxyl group (H-O) of chemisorbed water [32]. A single peak was observed at BE 399.6 eV in the N1s region in Fig. 3(c), indicating that nitrogen exists in the form of chemisorbed N_2 molecules or Ti-O-N bonds [33,34]. It can be seen that the Ti-O-N bonding is due to the interstitial site of N between the TiO_2 lattice [35]. The Ed3d spectrum in Fig. 3(d) showed peaks of $Eu3d_{5/2}$ (BE 1,125.1 eV and 1,134.1 eV) and $Eu3d_{3/2}$ (BE 1,154.2 eV and 1,164.3 eV). The peaks at BE 1,154.2 eV and 1,125.1 eV were generated by Eu^{2+} ions, and the peaks at 1,164.3 eV and 1,134.1 eV were due to Eu^{3+} ions; it was assumed that Eu exists as europium oxide on the TiO_2 surface [32, 36,37].

Table 1 lists the chemical composition of the photocatalysts calculated from EDS analysis. The precursor concentration used to precipitate nitrogen and europium was kept constant at 10 mM. The oxygen to titanium atomic ratio of bare TiO_2 was 66.9% : 33.1%, which is consistent with the quantitative value of TiO_2. N-TiO_2 and Eu-TiO_2, in which nitrogen and europium had precipitated on

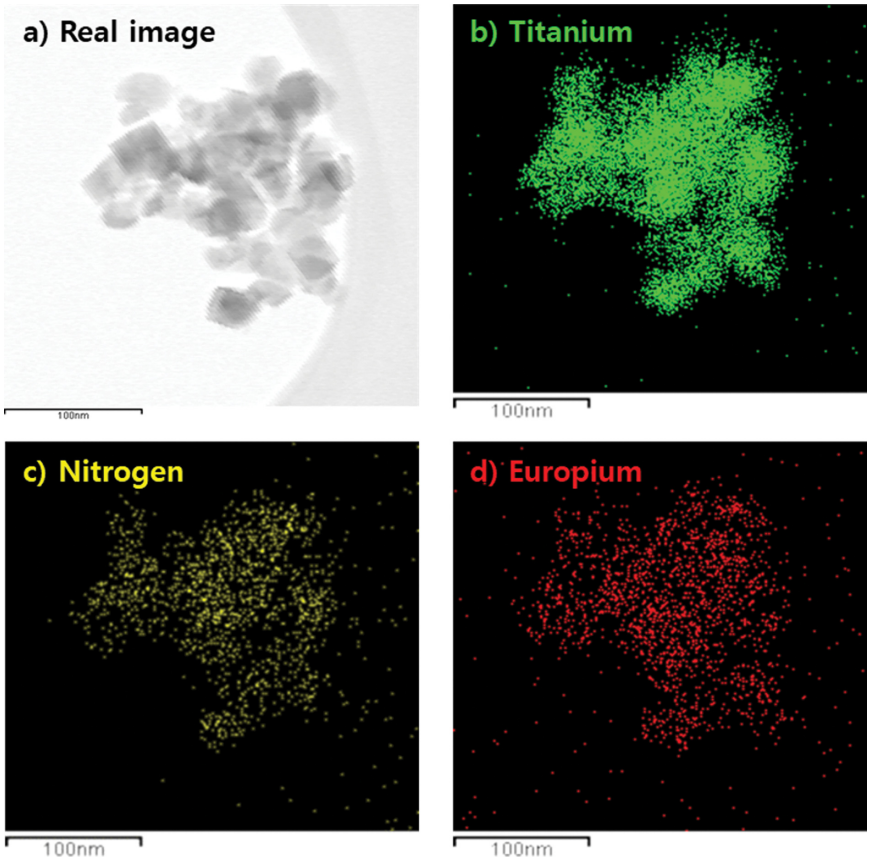

Fig. 2. HR-TEM real image (a) and mapped elements for titanium (b), nitrogen (c), and europium (d) in N/Eu codoped TiO_2 photocatalysts (MTP) prepared by PLP.

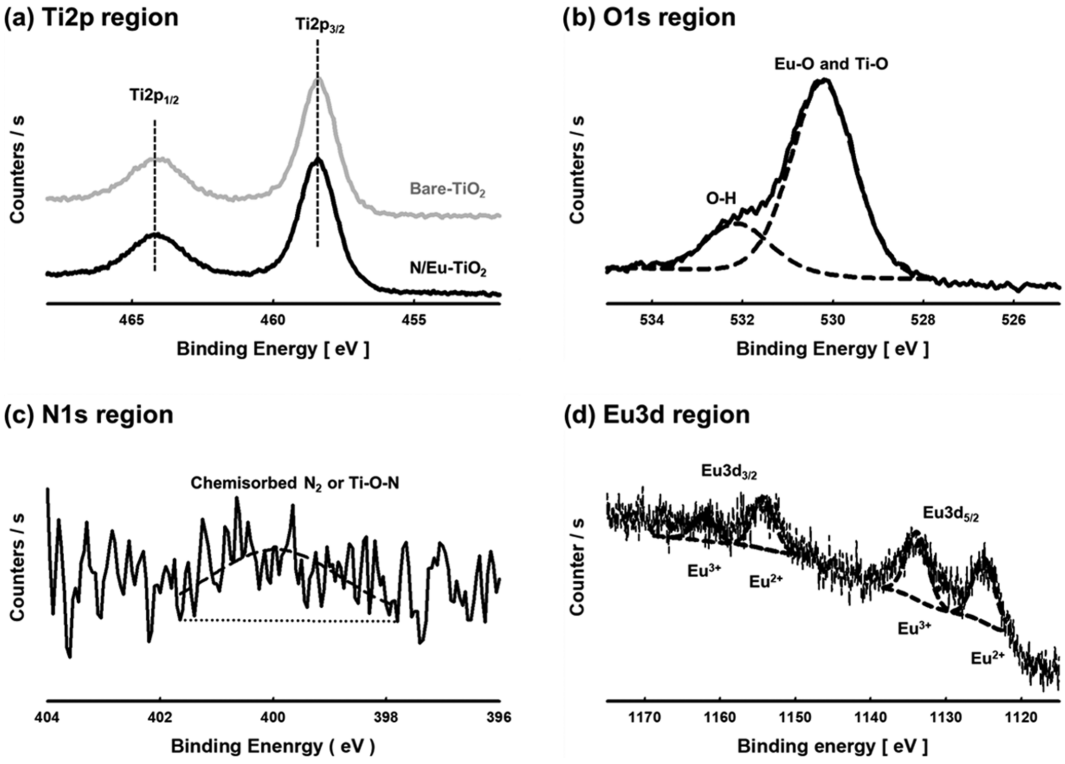

Fig. 3. High-resolution XPS spectra of N/Eu codoped TiO_2 photocatalysts prepared by PLP; Ti2p (a), O1s (b), N1s (c), and Eu3d region (d).

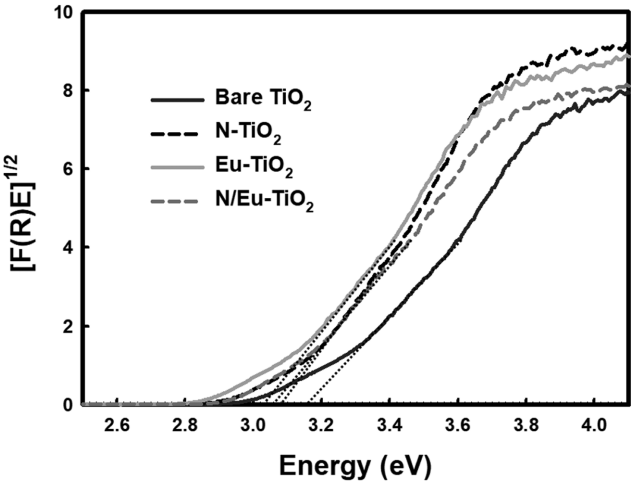

Fig. 4. Tauc plot for determining the bandgap of bare TiO_2 and MTPs.

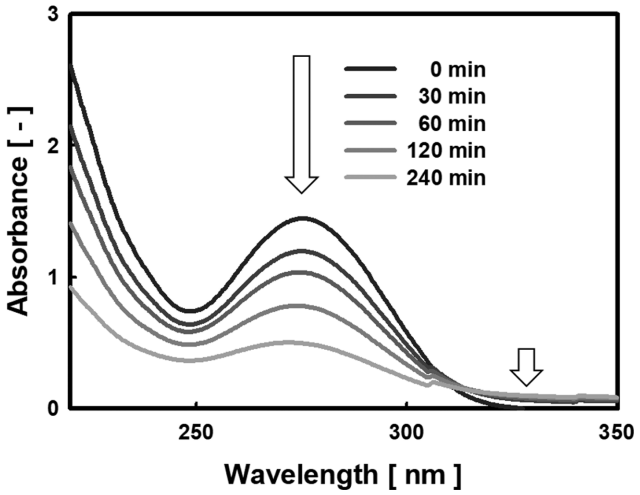

Fig. 5. Change in UV reflectance adsorption spectra according to the reaction time in the DCF decomposition reaction using UV LED lamp and MTP.

the TiO_2 powder, decreased the oxygen and titanium content and increased the nitrogen and europium composition. Even when nitrogen and europium precursors were added at the same concentration, the atomic composition of N was higher than that of Eu. Nitrogen and europium ions were reduced by electrons generated from PLP and adhering to the TiO_2 powder, which is consistent with the results in Fig. 2. Nitrogen and europium codoped N/Eu-TiO_2 also showed a similar tendency. Hence, the concentration of the added precursor affects the chemical composition of MTP.

The bandgap of MTPs, in which N and Eu were precipitated by PLP, was investigated by ultraviolet differential reflectance spectroscopy (UV-DRS) analysis. Fig. 4 shows the results of converting the measured UV-DRS spectrum of bare TiO_2 and MTPs to a Kubelka-Munk function. The bandgap of the TiO_2 powder used in this experiment was measured to be 3.16 eV, which is similar to the bandgap of the known TiO_2 powder. The bandgap of N-TiO_2 and Eu-TiO_2 with N and Eu deposited in the TiO_2 powder was 3.08 eV and 3.03 eV, respectively, which are lower than unmodified TiO_2 powder. It is presumed that the band gap is reduced because the impurity energy level is formed by nitrogen and europium precipitated in the TiO_2 powder [38,39]. The bandgap of N/Eu-TiO_2 was calculated to be 3.06 eV, which is less than N-TiO_2 but greater than Eu-TiO_2.

2. Photocatalytic Performance Evaluation

The photocatalytic performance of the modified photocatalysts prepared by PLP was examined from diclofenac sodium (DCF) decomposition, a representative antipyretic analgesic agent. In this experiment, a light source module was made using 100 UV and blue LEDs, and used in a photolysis reaction to evaluate the activity of MTPs. Fig. 5 shows the UV spectra obtained from the DCF decomposition reaction by MTP under the light source conditions using a UV LED lamp. Before starting the DCF decomposition reaction (reaction time=0 min), a band with a maximum absorption wavelength of 276 nm was observed, which was attributed to DCF [40]. Subsequently, as the reaction time increased, the absorbance decreased at the maximum absorption wavelength, indicating that the DCF decomposition reaction occurred by MTP. On the other hand, at a wavelength of 305 nm or more, the absorbance was higher than before the DCF decomposition reaction, which is due to by-product intermediates generated during DCF decomposition [41].

The DCF photolysis reaction was performed in an LED mod-

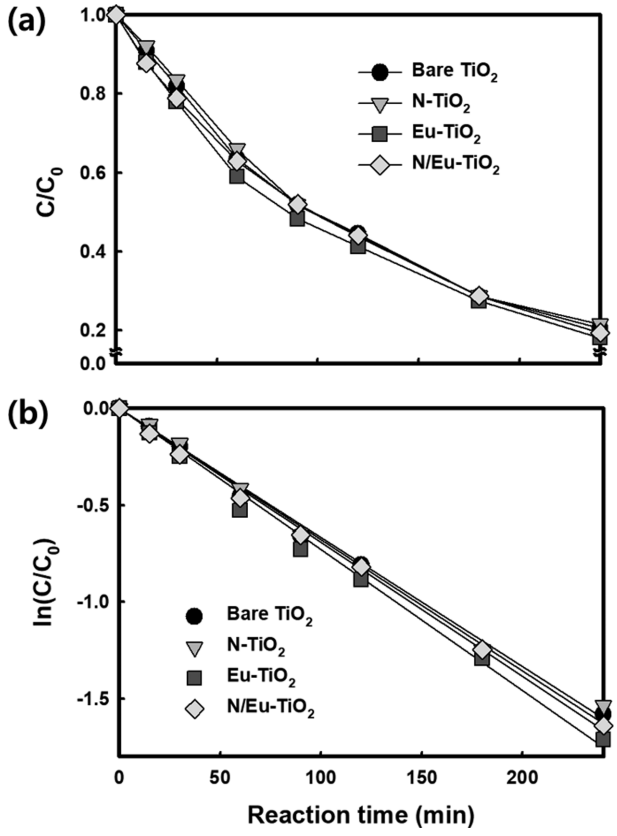

Fig. 6. C/C_0 plot (a) and first-order kinetics plot (b) of DCF decomposition reaction according to each photocatalyst type under UV light source (maximum wavelength 375 nm).

ule light source with bare TiO_2 and MTPs, and the activity of the photocatalysts was calculated assuming a first-order reaction rate. Fig. 6 presents the DCF decomposition pattern by each photocatalyst in the UV light source. Fig. 6(a) shows the change in DCF concentration (C/C_0) according to the reaction time. When reacted for 240 min using bare TiO_2, the DCF decomposition efficiency was approximately 79.42%. In the case of using N-TiO_2, approximately 78.46% of DCF was decomposed in a reaction time of 240 minutes, which was lower than that of bare TiO_2. In contrast, 81.93% and 80.59% of DCF were decomposed using Eu-TiO_2 and N/Eu-TiO_2, respectively, in 240 minutes, showing slightly improved DCF decomposition efficiency compared to unmodified TiO_2 photocatalyst. Fig. 6(b) shows the first-order kinetics plot of the DCF decomposition result obtained in Fig. 6(a). The DCF decomposition reaction constant k of unmodified TiO_2 photocatalyst was 6.79×10^{-3} min^{-1}. The first-order kinetics plot of N-TiO_2, Eu-TiO_2, and N/Eu-TiO_2 was 6.68×10^{-3} min^{-1}, 7.30×10^{-3} min^{-1}, and 6.92×10^{-3} min^{-1}, respectively. N-doped TiO_2 has a reduced bandgap compared to bare TiO_2. Hence, the N element present in TiO_2 acts as an electron-hole recombination center and an inhibitor of the DCF decomposition reaction [42,43]. On the other hand, the europium present in TiO_2 powder increases the DCF decomposition reaction rate by inhibiting electron-hole recombination of the photocatalyst [44]. N/Eu-TiO_2, in which N and Eu were precipitated together, decreased the recombination effect because of the lower N content than N-TiO_2. Moreover, the DCF decomposition reaction by Eu was improved, resulting in a higher decomposition rate constant than bare TiO_2.

Fig. 7 presents the C/C_0 plot and first-order kinetics plot of the DCF decomposition reaction under a visible light source (blue light LED), which is the visible light area. In Fig. 7(a), approximately 1.8% DCF decomposition occurred on bare TiO_2 after 240 min; hence, there was virtually no reaction, and the concentration of DCF only decreased due to adsorption on bare TiO_2. The MTPs prepared with PLP increased the DCF decomposition efficiency significantly compared to bare TiO_2. After 240 minutes of reaction time, the DCF decomposition efficiency of each MTP was the highest with Eu-TiO_2 (28.26%), followed in order by N/Eu-TiO_2 (27.11%) and N-TiO_2 (19.84%). Looking at the DCF decomposition rate constant obtained through the first-order kinetic plot in Fig. 7(b), the decomposition reaction rate constant k on unmodified TiO_2 was 5.84×10^{-5} min^{-1}. The DCF degradation reaction rate constant k on N-TiO_2 was 9.11×10^{-4} min^{-1}, which is a significant improvement over bare TiO_2, unlike under UV light conditions. The bandgap energy was reduced by the N generated on the TiO_2 surface, which enabled visible light adsorption, facilitating the generation of hydroxyl radicals by electrons in the conduction band [45,46]. In the case of Eu-TiO_2, k was 1.46×10^{-3} min^{-1}, showing the highest value. The bandgap was reduced by Eu precipitation, and the separation of electron-holes was increased using visible light. Hence, the amount of strong oxidants, such as hydroxyl radicals, was increased. This, in turn, increased the DCF degradation reaction rate [47]. The k of N/Eu-TiO_2 was 1.36×10^{-3} min^{-1}, which was significantly improved compared to that of N-TiO_2, which was close to the k value of Eu-TiO_2. From the result of Fig. 4, it can be seen that the band gap energy of N/Eu-TiO_2 was 3.06 eV, which was slightly decreased compared to that of N-TiO_2 (3.08 eV). However, the increase in electron-hole separation and the inhibition of recombination occur at the same time by N and Eu coexisting on the TiO_2 surface, showing that DCF decomposition reaction is actively carried out.

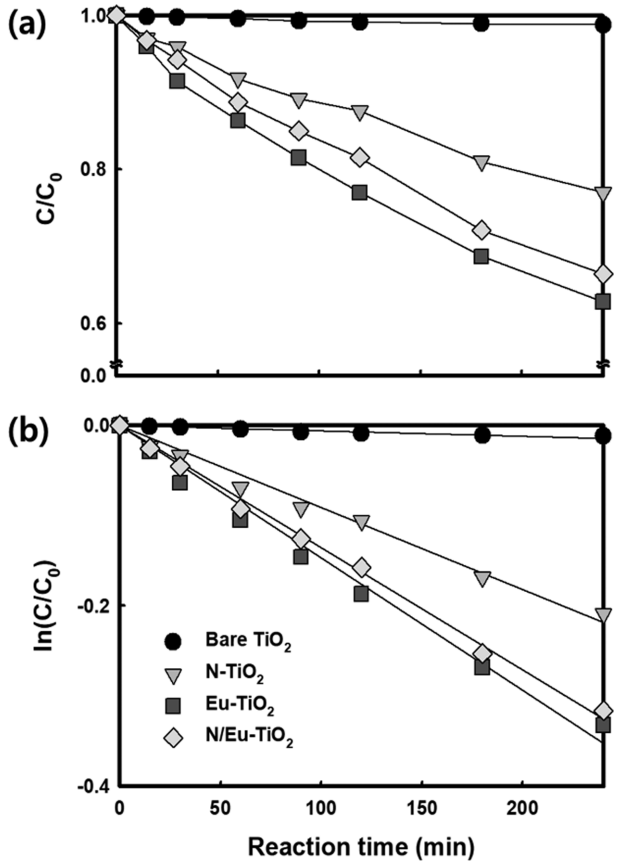

Fig. 7. C/C_0 plot (a) and first-order kinetics plot (b) of DCF decomposition reaction according to each photocatalyst type under blue light source (maximum wavelength 465 nm).

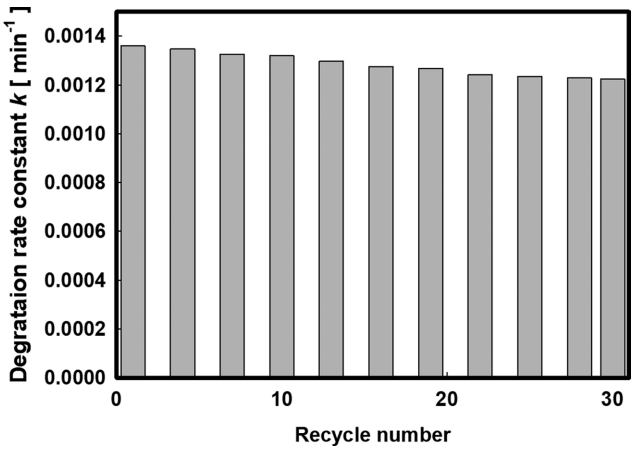

Fig. 8. DCF decomposition reaction rate constant change by the number of repeated uses of N/Eu-TiO_2 under visible light conditions.

N/Eu-TiO_2 was used as the photocatalyst to assess the reusability of the MTP prepared with PLP, and the DCF degradation reaction was repeated 30 times under visible light conditions. The photocatalyst powder was recovered and washed after each DCF decomposition experiment was completed and then naturally dried and used. Fig. 8 shows the rate constant k obtained through repeated decomposition experiments of DCF. After repeated use of 10 and 30 times, the DCF decomposition reaction rate constant k was approximately 3% and 10%, respectively, compared to the initial, and MTP prepared by PLP showed excellent reusability.

3. DCF Decomposition Reaction Mechanism

The mechanism of the degradation reaction of DCF by MTP was examined by measuring the intermediate products by liquid chromatography-mass spectrometry LC/MS, as summarized in Table 2. In this experiment, the Eu-TiO_2 photocatalyst and blue light source were used. Four representative by-products were observed in the DCF degradation reaction, as shown in Table 2.

Fig. 9 presents the degradation pathway of DCF based on the intermediate products detected in Table 2. DCF in the reaction solution undergoes decomposition by three pathways through hydrox-

Table 2. Intermediate-byproducts produced by DCF decomposition reaction

No.	m/z	Compound name	Chemical structure
1	296	2-(2,6-dichlorophenylamino) phenylacetic acid (Diclofenac)	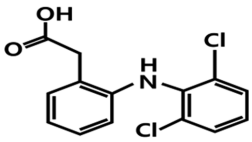
2	252	2-(2′,6′-dichlorphenylamino) methylbenzene	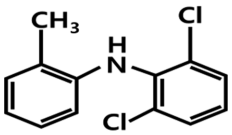
3	312	2-[(2,6-dichlorophenyl)amino]-5-hydroxy-benzeneacetic acid (5-hydroxydiclofenac)	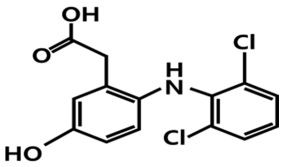
4	178	4-Amino-3,5-dichlorophenol	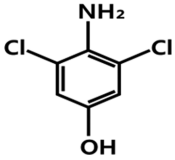

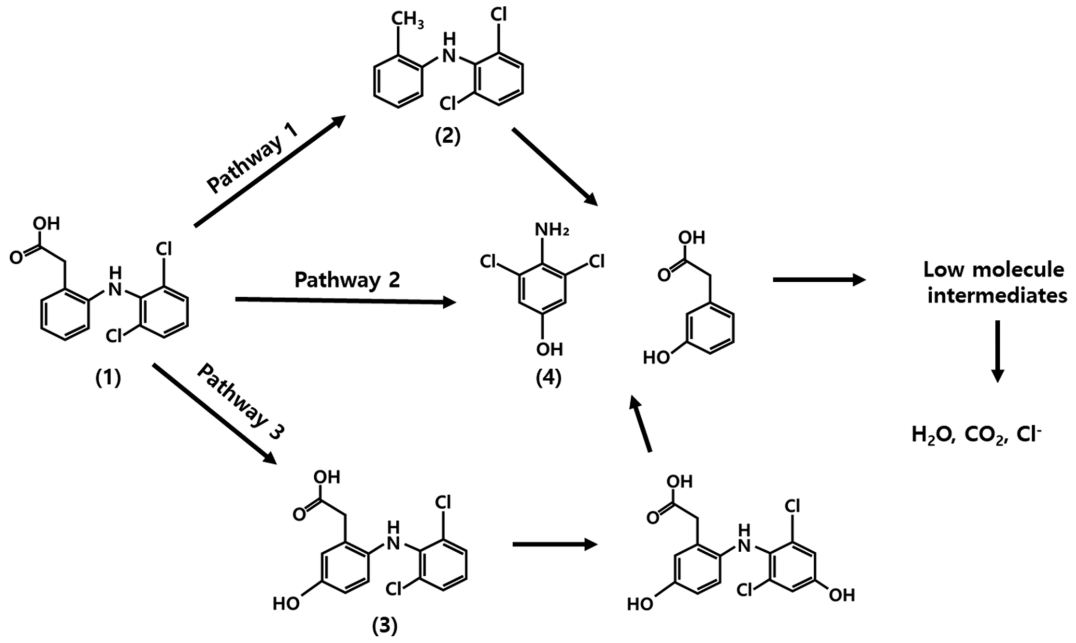

Fig. 9. Decomposition pathway of DCF by MTP (Eu-TiO_2) prepared by PLP.

ylation, decarboxylation, and C-N cleavage by photocatalysts [48, 49]. The first degradation reaction is the reaction by decarboxylation. The hydroxyl radicals generated by photocatalysis undergo a decarboxylation (elimination of -COO) reaction that attacks the CC bond of the acetic acid group in the DCF structure, and 2-(2′,6′-dichlorphenylamino) methylbenzene (2) is produced [6]. After that, cleavage of the C-N bond between the two aromatic rings and hydroxylation reaction occurs, and are changed into 4-amino-3,5-dichlorophenol (4) and 3-hydroxy-Benzeneacetic acid [48,50,51]. The second decomposition pathway is generated by direct cleavage and hydroxylation of the CN bond connecting the two aromatic rings of the DCF structure, and by this, 4-amino-3,5-dichlorophenol (4) and 3-hydroxy-Benzeneacetic acid is produced [49, 50]. As a third decomposition pathway, hydroxylation occurs through the addition of an electrophilic hydroxyl radical to the aromatic ring and changes to 5-hydroxydiclofenac (3) with an increased m/z value of 16 [6,51,52]. Then, after di-hydroxylation, C-N bond cleavage occurs and changes to 4-amino-3,5-dichlorophenol (4) [49]. It is finally mineralized into water, carbon dioxide, and chlorine through a mechanism involving ring-opening [48,53].

CONCLUSIONS

This study investigated the physicochemical properties and photocatalyst performance of visible light response TiO_2 photocatalysts doped with N and Eu were prepared by PLP. A modified photocatalyst with activity in visible light was prepared by precipitating nitrogen and europium on TiO_2 powder using PLP. The activity of the prepared MTP was assessed by the decomposition of diclofenac, a pharmaceutical ingredient, and compared and evaluated with bare TiO_2 photocatalysts. The dopant was precipitated in proportion to the precursor amount, but more nitrogen was precipitated than europium even when the same amount was added. TEM showed that nitrogen and europium were dispersed uniformly over the TiO_2 surface. High-resolution XPS showed that the Ti2p peak positions of MTP precipitated with N and Eu coincided with bare TiO_2, and europium precipitated in the form of europium oxide. The bandgap of MTP was lower than that of bare TiO_2, and MTP that precipitated only europium showed the lowest value. In the DCF decomposition reaction using visible light, the efficiency of all MTPs was superior to that of the bare TiO_2 photocatalysts. In particular, the efficiency of the photocatalyst precipitating as europium was the best. On the other hand, the photocatalyst, in which only nitrogen had precipitated, was less active than the photocatalyst, in which nitrogen and europium were simultaneously precipitated. In evaluating the reusability of MTPs, which were used repeatedly (30 times) in blue light, the DCF degradation reaction rate constant k decreased by approximately 10%. In the decomposition of DCF using MTPs, four by-products were detected by LC/MS. Three pathways were considered: hydroxylation, decarboxylation, and C-N cleavage. DCF was eventually mineralized to H_2O, CO_2, and chlorine ions by hydroxylation by oxidizing agents, such as OH, produced in MTP. Through this study, the visible light responsive TiO_2 manufactured using simple and effective PLP shows that it can be applied as a drug component removal technology known as a difficult-to-decompose material.

ACKNOWLEDGEMENTS

This work was supported by the National Research Foundation of Korea (NRF) grant funded by the Korean Government (MSIT) (2021R1A2C1006315).

REFERENCES

1. K. A. Holloway, *Expert Rev. Clin. Pharmacol.*, **4**, 335 (2011).
2. J. Busfield, *Soc. Sci. Med.*, **131**, 199 (2015).
3. T. aus der Beek, F.-A. Weber, A. Bergmann, S. Hickmann, I. Ebert, A. Hein and A. Küster, *Environ. Toxicol. Chem.*, **35**, 823 (2016).
4. G. E. Swan, R. Cuthbert, M. Quevedo, R. E. Green, D. J. Pain, P. Bartels, A. A. Cunningham, N. Duncan, A. A. Meharg, J. L. Oaks, J. P. Jones, S. Shultz, M. A. Taggart, G. Verdoorn and K. Wolter, *Biol. Lett.*, **2**, 279 (2006).
5. R. Triebskorn, H. Casper, A. Heyd, R. Eikemper, H.-R. Köhler and J. Schwaiger, *Aquat. Toxicol.*, **68**, 151 (2004).
6. L. Zhang, Y. Liu and Y. Fu, *RSC Adv.*, **10**, 9907 (2020).
7. D. Kanakaraju, C. A. Motti, B. D. Glass and M. Oelgemoller, *Environ. Chem.*, **11**, 51 (2014).
8. M. Irandost, R. Akbarzadeh, M. Pirsaheb, A. Asadi, P. Mohammadi and M. Sillanpaa, *J. Mol. Liq.*, **291**, 111342 (2019).
9. X. Lu, Y. Shao, N. Gao, J. Chen, Y. Zhang, H. Xiang and Y. Guo, *Ecotoxicol. Environ. Saf.*, **141**, 139 (2017).
10. S. J. Ki, K. J. Jeon, Y. K. Park, S. Jeong, H. Lee and S. C. Jung, *Catal. Today*, **293**, 15 (2017).
11. H. Lee, S. H. Park, Y. K. Park, S. J. Kim, S. G. Seo, S. J. Ki and S. C. Jung, *Chem. Eng. J.*, **278**, 259 (2015).
12. S. C. Jung, *Water Sci. Technol.*, **63**, 1491 (2011).
13. D. J. Lee, Y. K. Park, S. J. Kim, H. Lee and S. C. Jung, *Korean J. Chem. Eng.*, **32**, 1188 (2015).
14. Z. Hua, Z. Dai, X. Bai, Z. Ye, H. Gua and X. Huang, *J. Hazard. Mater.*, **293**, 112 (2015).
15. H. Lee, Y. K. Park, S. J. Kim, B. H. Kim and S. C. Jung, *J. Ind. Eng. Chem.*, **32**, 259 (2015).
16. Y. Zhang and Q. Li, *Solid State Sci.*, **16**, 16 (2013).
17. S. J. Ki, Y. K. Park, J. S. Kim, W. J. Lee, H. Lee and S. C. Jung, *Chem. Eng. J.*, **377**, 120087 (2019).
18. H. Lee, I. S. Park, H. J. Bang, Y. K. Park, H. Kim, H. H. Ha, B. J. Kim and S. C. Jung, *Appl. Surf. Sci.*, **471**, 893 (2019).
19. H. Lee, I. S. Park, H. J. Bang, Y. K. Park, E. B. Cho, B. J. Kim and S. C. Jung, *Appl. Surf. Sci.*, **481**, 625 (2019).
20. S. C. Kim, Y. K. Park and S. C. Jung, *Korean J. Chem. Eng.*, **38**, 885 (2021).
21. K. H. Chung, S. Jeong, H. Lee, S. J. Kim, K. J. Jeon, Y. K. Park and S. C. Jung, *Int. J. Hydrogen Energy*, **42**, 24099 (2017).
22. H. Lee, S. H. Park, S. G. Seo, S. J. Kim, S. C. Kim, Y. K. Park and S. C. Jung, *Curr. Nanosci.*, **10**, 7 (2014).
23. S. C. Kim, Y. K. Park, B. H. Kim, H. Kim, W. J. Lee, H. Lee and S. C. Jung, *Korean J. Chem. Eng.*, **35**, 750 (2018).
24. S. Jeong, K. H. Chung, H. Lee, H. Park, K. J. Jeon, Y. K. Park and S. C. Jung, *ACS Sustain. Chem. Eng.*, **5**, 3659 (2017).
25. H. Lee, B. H. Kim, Y. K. Park, K. H. An, Y. J. Choi and S. C. Jung, *Int. J. Hydrogen Energy*, **41**, 7582 (2016).
26. M. K. Mun, W. O. Lee, J. W. Park, D. S. Kim, G. Y. Yeom and D. W.

Kim, *Appl. Sci. Converg. Technol.*, **26**, 164 (2017).
27. S. Pitchaimuthu, K. Honda, S. Suzuki, A. Naito, N. Suzuki, K. Katsumata, K. Nakata, N. Ishida, N. Kitamura, Y. Idemoto, T. Kondo, M. Yuasa, O. Takai, T. Ueno, N. Saito, A. Fujishima and C. Terashima, *ACS Omega*, **3**, 898 (2018).
28. Y. K. Heo, M. A. Bratescu, T. Ueno and N. Saito, *J. Appl. Phys.*, **116**, 024302 (2014).
29. D. Ihnatiuk, C. Tossi, I. Tittonen and O. Linnik, *Catalysts*, **10**, 1074 (2020).
30. S. Anwer, G. Bharath, S. Iqbal, H. Qian, T. Masood, K. Liao, W. J. Cantwell, J. Zhang and L. Zheng, *Electrochim. Acta*, **283**, 1095 (2018).
31. J. Tian, H. Gao, H. Kong, P. Yang, W. Zhang and J. Chu, *Nanoscale Res. Lett.*, **8**, 533 (2013).
32. I. Camps, M. Borlaf, M. T. Colomer, R. Moreno, L. Duta, C. Nita, A. Perez del Pino, C. Logofatu, R. Serna and E. Gyorgy, *RSC Adv.*, **7**, 37643 (2017).
33. D. Chen, Z. Jiang, J. Geng, Q. Wang and D. Yang, *Ind. Eng. Chem. Res.*, **46**, 2741 (2007).
34. G. Yan, M. Zhang, J. Hou and J. Yang, *Mater. Chem. Phys.*, **129**, 553 (2011).
35. T. T. Khan, G. A. K. M. R. Bari, H. J. Kang, T. G. Lee, J. W. Park, H. J. Hwang, S. M. Hossain, J. S. Mun, N. Suzuki, A. Fujishima, J. H. Kim, H. K. Shon and Y. S. Jun, *Catalysts*, **11**, 109 (2021).
36. W. Q. Liu, D. Wu, H. Chang, R. X. Duan, W. J. Wu, G. Amu, K. F. Chao, F. Q. Bao and O. Tegus, *Nanomaterials*, **8**, 66 (2018).
37. C. H. Zeng, K. Zheng, K. L. Lou, X. T. Meng, Z. Q. Yan, Z. N. Ye, R. R. Su and S. Zhong, *Electrochim. Acta,* **165**, 396 (2015).
38. S. A. Ansari, M. M. Khan, M. O. Ansari and M. H. Cho, *New J. Chem.*, **40**, 3000 (2016).
39. M. Myilsamy, M. Mahalakshmi, N. Subha, A. Rajabhuvaneswari and V. Murugesan, *RSC Adv.*, **6**, 35024 (2016).
40. L. Rizzo, S. Meric, D. Kassinos, M. Guida, F. Russo and V. Belgiorno, *Water Res.*, **43**, 979 (2009).
41. B. Di Credico, R. Bellobono, M. D'Arienzo, D. Fumagalli, M. Redaelli, R. Scotti and F. Morazzoni, *Int. J. Photoenergy*, **2015**, 919217 (2015).
42. L. A. M. Lx, A. E. González, S. Cipagauta-Díaz and R. Gómez, *J. Chem. Technol. Biotechnol.*, **95**, 2694 (2020).
43. J. Wang, D. N. Tafen, J. P. Lewis, Z. Hong, A. Manivannan, M. Zhi, M. Li and N. Wu, *J. Am. Chem. Soc.*, **131**, 12290 (2009).
44. D. Chen, Q. Zhu, Z. Lv, X. Deng, F. Zhou and Y. Deng, *Mater. Res. Bull.*, **47**, 3129 (2012).
45. S. Ramandi, M. H. Entezari and N. Ghows, *Ultrason. Sonochem.*, **38**, 234 (2017).
46. T. P. Nguyen, Q. B. Tran, Q. V. Ly, L. T. Hai, D. T. Le, M. B. Tran, T. T. T. Ho, X. C. Nguyen, M. Shokouhimehr, D. V. N. Vo, S. S. Lam, H. T. Do, S. Y. Kim, T. V. Tung and Q. V. Le, *Arab. J. Chem.*, **13**, 8361 (2020).
47. J. Xu, Y. Ao, D. Fu and C. Yuan, *J. Colloid Interface Sci.*, **328**, 447 (2008).
48. Z. Hu, X. Cai, Z. Wang, S. Li, Z. Wang and X. Xie, *J. Hazard. Mater.*, **380**, 120812 (2019).
49. H. Shi, G. Zhou, Y. Liu, Y. Fu, H. Wang and P. Wu, *RSC Adv.*, **9**, 31370 (2019).
50. I. Michael, A. Achilleos, D. Lambropoulou, V. Osorio Torrens, S. Pérez, M. Petrovic, D. Barceló and D. Fatta-Kassinos, *Appl. Catal. B*, **147**, 1015 (2014).
51. E. Nie, M. Yang, D. Wang, X. Yang, X. Luo and Z. Zheng, *Chemosphere*, **113**, 165 (2014).
52. H. Yu, E. Nie, J. Xu, S. Yan, W. J. Cooper and W. Song, *Water Res.*, **47**, 1909 (2013).
53. S. Salaeh, D. J. Perisic, M. Biosic, H. Kusic, S. Babic, U. L. Stangar, D. D. Dionysiou and A. L. Bozic, *Chem. Eng. J.*, **304**, 289 (2016).